AGU PUBLICATIONS

Geophysical Research Letters

RESEARCH LETTER
10.1002/2013GL058601

Key Points:
- First experiments on basalts at seismic slip rates
- Interstitial glass renders the basalts more prone to frictional instabilities
- Interstitial glass in basalts increases the steady-state friction

Supporting Information:
- Read me
- The supporting information includes text, figures and tables divided in three supplementary items

Correspondence to:
M. Violay,
marie.violay@erdw.ethz.ch

Citation:
Violay, M., G. Di Toro, B. Gibert, S. Nielsen, E. Spagnuolo, P. Del Gaudio, P. Azais, and P. G. Scarlato (2014), Effect of glass on the frictional behavior of basalts at seismic slip rates, *Geophys. Res. Lett.*, *41*, 348–355, doi:10.1002/2013GL058601.

Received 5 NOV 2013
Accepted 27 DEC 2013
Accepted article online 4 JAN 2014
Published online 22 JAN 2014

Effect of glass on the frictional behavior of basalts at seismic slip rates

M. Violay[1,2], G. Di Toro[1,3], B. Gibert[4], S. Nielsen[1,5], E. Spagnuolo[1], P. Del Gaudio[1], P. Azais[4], and P. G. Scarlato[1]

[1]Istituto Nazionale di Geofisica e Vulcanologia, Rome, Italy, [2]Now at Geologisches Institut, ETHZ Zürich, Zürich, Switzerland, [3]Dipartimento di Geoscienze, Università degli Studi di Padova, Padua, Italy, [4]Géosciences Montpellier, UMR 5243, Université Montpellier II, Montpellier, France, [5]Earth Sciences, University of Durham, Durham, UK

Abstract We performed 31 friction experiments on glassy basalts (GB) and glass-free basalts (GFB) at slip rates up to 6.5 m s^{-1} and normal stress up to 40 MPa (seismic conditions). Frictional weakening was associated to bulk frictional melting and lubrication. The weakening distance (D_w) was about 3 times shorter in GB than in GFB, but the steady state friction was systematically higher in GB than in GFB. The shorter D_w in GB may be explained by the thermal softening occurring at the glass transition temperature (T_g ~500°C), which is lower than the bulk melting temperature (T_m ~1250°C) of GFB. Postexperiment microanalyses suggest that the larger crystal fraction measured in GB melts results in the higher steady state friction value compared to the GFB melts. The effect of interstitial glass is to facilitate frictional instability and rupture propagation in GB with respect to GFB.

1. Introduction

The determination of frictional evolution of rocks with slip and slip rate is of paramount importance in earthquake physics. Friction controls, for instance, rupture nucleation and propagation, the static and dynamic stress drops, and the frictional heat generated during slips [*Scholz*, 2002; *Di Toro et al*., 2011]. Although basaltic rocks are common in active tectonic environments (continental rifts and traps, oceanic transform faults and ridges, volcanoes, etc.) and cover more than 60% of the Earth's surface, data on their frictional properties under seismic deformations conditions are limited. To date, high-velocity friction experiments have been conducted primarily on intrusive igneous rocks (mainly gabbro) indicating that frictional melt lubrication develops which controls friction [*Shimamoto and Lin*, 1994; *Tsutsumi and Shimamoto*, 1997; *Hirose and Shimamoto*, 2005; *Di Toro et al*., 2006; *Mizoguchi et al*., 2006; *Tsutsumi and Mizoguchi*, 2007; *Nielsen et al*., 2008; *Niemeijer et al*., 2011]. Frictional melting occurs also in extrusive rocks (andesites, basalts, etc.), which have been poorly investigated so far [*Lavallée et al*., 2012] and where the presence of interstitial glass introduces a higher degree of complexity. Here, we study the effect of an initially present interstitial glass on friction by conducting comparative experiments on glassy basalts (GB) and glass-free basalts (GFB). We use the rotary shear machine, named SHIVA (Slow to High Velocity Apparatus) installed at the High Pressure High Temperature Laboratory of Istituto Nazionale di Geofisica e Vulcanologia (INGV), Rome (Italy).

2. Methods

2.1. Experimental and Analytical Methods

Thirty-one experiments were performed with SHIVA (Table S1 in the supporting information). Thanks to the large power available (up to 300 kW), SHIVA imposes on the specimen's quite realistic seismic deformation conditions in terms of stress, velocity, and acceleration. SHIVA uses two brushless engines in a rotary shear configuration to slide hollow rock cylinders (50/30 mm extrusive/intrusive diameter) at (1) nominally infinite displacement, (2) slip rates V ranging from 10 μm s^{-1} to 6.5 m s^{-1}, and (3) accelerations up to 65 m s^{-2}. An air actuator allows maintaining the normal stresses σ_n up to 40 MPa during the sliding (for details on the apparatus, the control and acquisition system, etc., see *Di Toro et al*. [2010] and *Niemeijer et al*. [2011]). Mechanical data (axial load, torque, axial displacement, and angular rotation) are acquired at a frequency up to 25 kHz. Slip, slip rate, and shear stress are determined using methods outlined in *Tsutsumi and Shimamoto* [1997] and *Di Toro et al*. [2010]. Samples are prepared following the procedure described in *Nielsen et al*. [2012], which ensures

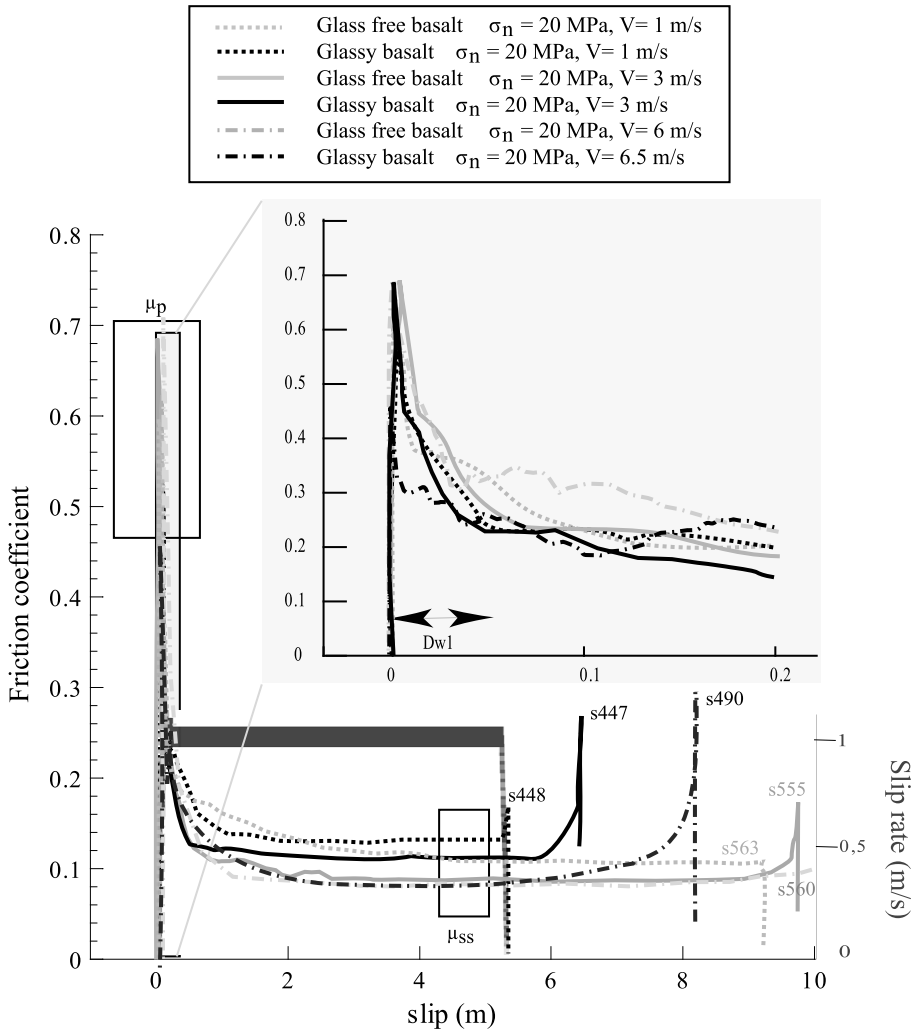

Figure 1. Friction coefficient versus slip for glassy basalt (GB) and glass-free basalt (GFB). The experiments were performed at target slip rate $V = 1\ m\ s^{-1}$ (grey dotted line = GFB, s563; black dotted line = GB, s448), $V = 3\ m\ s^{-1}$ (grey solid line = GFB, s555; black solid line = GB, s447,), $V = 6$ m/s, 6.5 m/s (grey dashed line = GFB; s560, black dashed line = GB, s490), acceleration = $7.8\ m\ s^{-2}$, and $\sigma_n = 20$ MPa. The velocity curve of GB experiment s448 is in grey. The inset highlights the first 30 cm of slip for these experiments. Given the same experimental conditions (V, σ_n, and acceleration), D_w is shorter and τ_{ss} higher for GB than GFB, respectively.

good parallelism of the sliding surfaces (sample misalignment $< 1\ \mu m$) avoiding the pregrinding after sample installation in the machine.

In all the experiments, we first loaded the sample to the target normal stress and then imposed a trapezoidal velocity function (acceleration to the target slip rate, steady state slip rate, deceleration, and slip arrest, Figure 1). Posttested samples were impregnated with epoxy and cut perpendicular to the slip surface and tangential to the slip direction for microstructural and microanalytical investigations carried out under optical microscopes, energy dispersive spectroscopy-equipped field emission scanning electron microscope (EDS-FESEM, INGV, Rome) and electron probe microanalyzer (EPMA, INGV, Rome).

The bulk viscosity of the friction melt (liquid + crystal fraction) during the steady state frictional sliding was modeled in two steps: (1) estimate the viscosity of the liquid fraction using the measured chemical composition (EPMA data) and temperature (measured with a thermocouple) (see Figure S1) and constrained by microstructural data as input parameters for the viscosity calculator by *Giordano et al.* [2008] and (2) estimate the rheological effect of the measured crystal fraction (image analysis performed with Adobe Photoshop software) using the viscosity calculator by *Costa et al.* [2009].

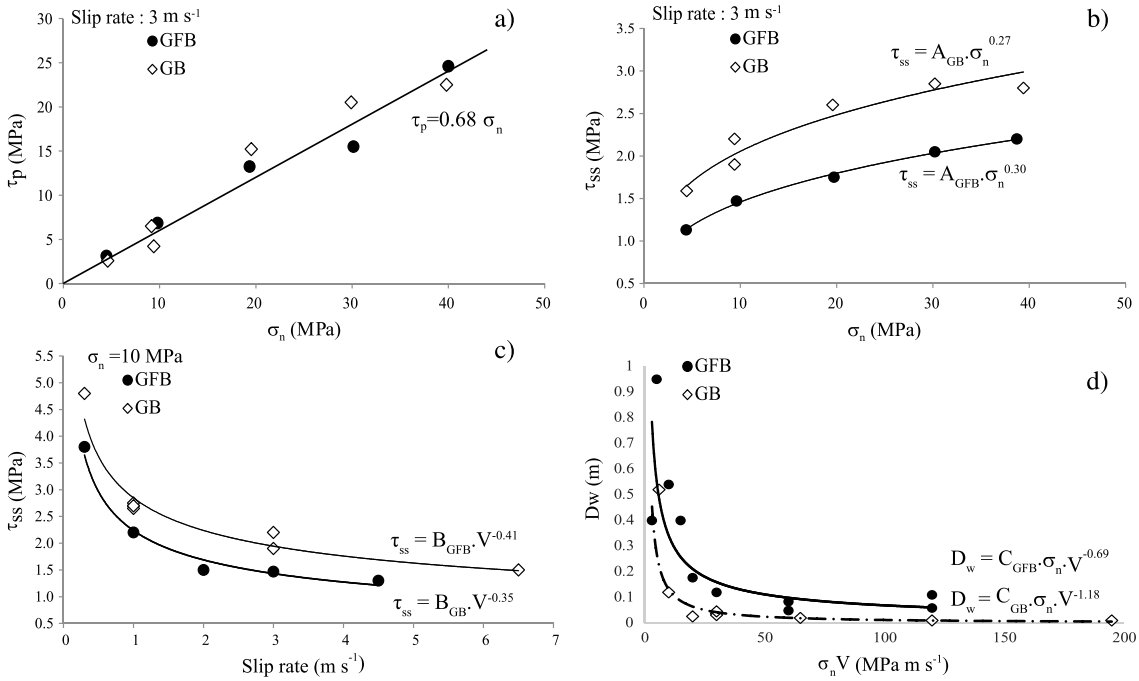

Figure 2. Shear stress and weakening distance for varying normal stress and velocity. Acceleration is 7.8 m s^{-2} for all shown data. (a) Peak (τ_p) and (b) steady state (τ_{ss}) shear stress as a function of the imposed normal stress with unvaried target velocity $V = 3$ m s^{-1}. (c) Steady state shear stress (τ_{ss}) as a function of the imposed target velocity with unvaried normal stress $\sigma_n = 10$ MPa. (d) D_w as a function of $\sigma_n V$ (in MW m^{-2}). D_w data are shown for 21 experiments where the exponential decay curve had a best fit coefficient $R^2 \geq 0.9$ (see Table S1).

2.2. Glassy and Glass-Free Basalts Petrography

The two basalt rocks were selected for their similar porosity (<3%) and grain size (100 μm) but different glass content (GB versus GFB) (Table S1; for chemical composition of the rocks see Table S2 and *Violay et al.* [2012]).

The GB from the cap rock of the Deves lava flow (Sénouire Valley, France) is a porphyritic basalt containing about 20 vol % phenocrysts of clinopyroxene and olivine in a groundmass made of phonolitic glass (15–25 vol % of the total rock) and fine-grained (< 100 μm) plagioclase (24–32 vol %), clinopyroxene (32–40 vol %), and oxides (4–8 vol %). This modal composition is uniformly distributed at the thin-section scale. The GB samples contain 0.6 wt % volatiles (thermogravimetric measurements up to 1200°C).

The GFB from the Escandorgue flow (Languedoc-Roussillon, France) is a microcrystalline to cryptocrystalline basalt containing about 5 vol % phenocrysts of clinopyroxenes and (few) olivines in a fine-grained (< 100 μm) homogenous groundmass made of plagioclase (35–45 vol %), clinopyroxene (25–35%), feldspathoids (10%), and titanomagnetite (5–15%). The GFB samples do not contain volatiles (thermogravimetric measurements up to 1200°C).

3. Results

3.1. Mechanical Data

In all experiments, once the velocity function was applied, the apparatus initially deformed elastically (i.e., shear stress increased linearly with time, not shown in Figure 1) until the static friction was overcome and the samples started to slide (Figure 1). The friction coefficient ($\mu = \tau/\sigma_n$ with τ shear stress and σ_n normal stress) decayed from a peak value $\mu_{p\ GFB} = 0.65 \pm 0.04$ and $\mu_{p\ GB} = 0.56 \pm 0.17$ (respectively for GB and GFB) to a steady state value $\mu_{ss\ GFB} = 0.15 \pm 0.11$ and $\mu_{ss\ GB} = 0.21 \pm 0.18$ (respectively for GB and GFB) over a weakening distance D_w (Figure 1). For both GB and GFB, the exponential decay of shear stress with slip δ is described by $\tau = \tau_{ss} + (\tau_p - \tau_{ss}) \exp((-\delta/D_w)^{\alpha})$ where α is a constant (subscripts ss and p stand for steady state and peak, respectively; the equation was modified from *Han et al.* [2010]). For the same acceleration (7.8 m s^{-2}) and applied normal stress (e.g., 20 MPa), D_w (1) was shorter for GB than GFB (compare grey with black curves in

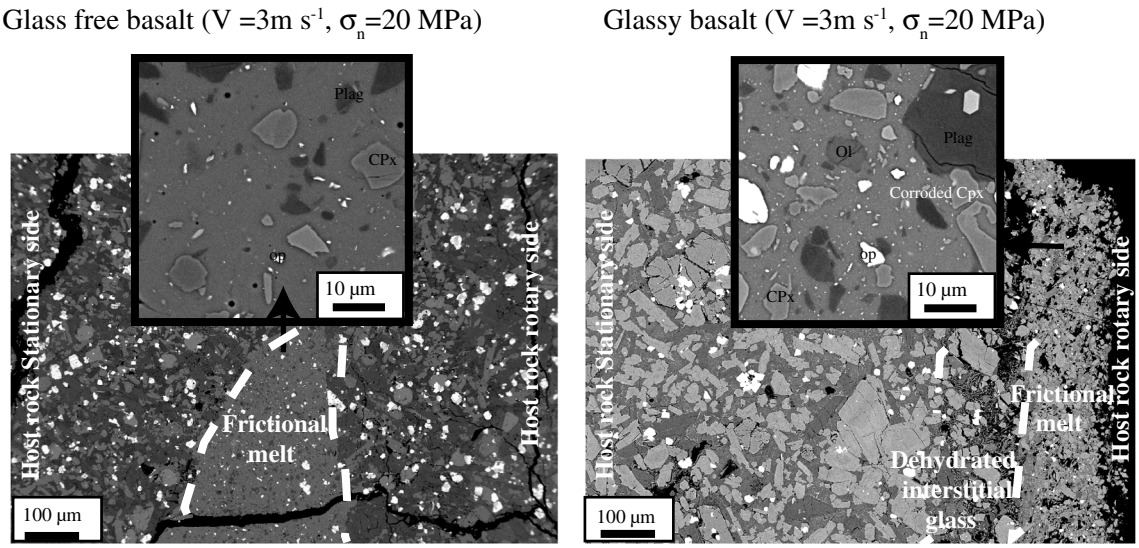

Figure 3. Slip zones of GB and GFB after steady state friction was achieved (> 1 m of slip). Samples were deformed at $\sigma_n = 20$ MPa and $V = 3$ m s^{-1}. At the end of the experiments, both basalts had the wall rocks separated by a continuous layer of glass. Survivor clasts were more abundant in GB (~50 ± 4% in volume) than in the GFB (~25 ± 4% in volume). Acronyms: Gl: glass, Pl: plagioclase, CPx: clinopyroxene, Ol: olivine, Op: Opaque. FE-SEM backscattered electron images.

inset of Figure 1) and (2) decreased with increasing target slip rate (compare solid with dashed and dotted curves in inset of Figure 1). The peak friction coefficient was not significantly influenced by the type of basalt, whereas steady state friction coefficient was about 30% lower for GFB than for GB at a given slip rate (Figures 1, 2a, and 2b). The peak shear stress increased approximately linearly with normal stress according to Byerlee's friction law (Figure 2a). Instead, the normal stress had a nonlinear effect on the magnitude of shear stress at steady state, described by a best fit curve of the form $\tau_{ss} = A_{GB}\,\sigma_n^{0.27}$ for GB and $\tau_{ss} = A_{GFB}\,\sigma_n^{0.30}$ for GFB (A is a constant) (Figure 2b). The shear stress dependence with slip rate at the steady state is described by a best fit curve of the form $\tau_{ss} = B_{GB}V^{-0.35}$ for GB and $\tau_{ss} = B_{GFB}V^{-0.41}$ for GFB (B is a constant) (Figure 2c). For both rocks, D_w decreased with $\sigma_n V$ (Figure 2) according to a best fit curve of the form $D_w = C_{GB}\,(\sigma_n V)^{-1.18}$ for GB and $D_w = C_{GFB}\,(\sigma_n V)^{-0.69}$ for GFB (C is a constant) (Figure 2d). Sample shortening rate was constant after the initial transient and depended on the target velocity and applied normal stress, as argued by *Nielsen et al.* [2008], the shortening rate is proportional to the frictional power ($\Phi = \mu_{ss}\,\sigma_n\,V$ in W m^{-2}) dissipated at steady state (assuming no significant radiation loss). Here, the measured shortening rate was (depending on ϕ and for $\sigma_n > 10$ MPa, and $V > 1$ m s^{-1}) 0.6 ± 0.1 mm/m of slip for GB sample and 0.3 ± 0.05 mm/m of slip for the GFB sample (Table S1). From *Nielsen et al.* [2008, equation (11)] and considering typical constitutive parameters for basalt (specific heat capacity = 949 J (kg C)$^{-1}$, latent heat = 350 10^3 J kg^{-1}, mass density = 2900 kg m^{-3}, measured melt temperature (by thermocouple) of ~1250°C for GFB (Figure S1)), we predict a shortening rate of 0.25 mm/m at $V = 1$ m s^{-1} which is consistent with the GFB shortening measurements.

3.2. Microstructural and Microanalytical Data

For GFB samples, at the end of experiments performed at $\sigma_n^{eff} = 20$ MPa and $V = 3$ m s^{-1}, the wall rocks were separated by a continuous 100–200 µm thick layer of glass (Figure 3a). From the two-dimensional analysis of SEM backscattered electron images of the glass layer we estimated < 1% in volume of vesicles and a ~25 ± 4% in volume of survivor clasts (< 10 µm in size). Clinopyroxene and plagioclase crystals were corroded, which indicates heating above the liquidus temperature of labradorite (1200°C). Olivine crystals showed pseudo euhedral shape suggesting a temperature below the liquidus temperature of the olivine (1400°C). Independently of the experimental conditions, in all the slipping zones produced at steady state, the composition of the glass was almost identical (within the EPMA resolution) to the bulk composition of the initial GFB (X-ray fluorescence analysis, Table S1) [*Violay et al.*, 2012]. This indicates that the GFB melt resulted from "total melting" of the wall rocks. From microstructural evidences and thermocouple measurements at the steady state (Figure S1), we estimated a melt temperature of ~1250 ± 100°C.

For GB samples at the end of experiments performed at $\sigma_n^{eff} = 20$ MPa and $V = 3$ m s^{-1}, the wall rocks were separated by a continuous, 150–250 μm thick layer of glass (Figure 3). The initial (interstitial) glass dehydrated next to the newly formed layer of glass. From the 2-dimensional analysis of SEM images of the glass layer, we estimated up to 10% in volume of vesicles and ~50 ± 4% in volume of survivor clasts (from 1 to 50 μm in size). Olivine, clinopyroxene, and plagioclase clasts had pseudo euhedral shape (no evidence of thermal corrosion) which indicates a temperature below the liquidus of clinopyroxene (~1100°C). In all experiments where the steady state conditions were achieved, the slipping zone had the composition of the glass intermediate between the bulk composition of the initial GB rock (X-ray fluorescence analysis) and the composition on the interstitial phonolitic glass (EPMA analysis) (Table S1) [*Violay et al.*, 2012]. The absence of corrosion in the clasts and the intermediate composition of the newly formed glass suggest that the GB melt was formed by selective melting of the wall rocks. The larger clast fraction measured after experiments in GB rocks is probably due to the lower temperature (~1050°C) achieved by the GB melt compared to the GFB melt (~1250°C). From microstructural evidences and thermocouple measurements at the steady state, we estimated an average melt temperature of ~1050 ± 100°C (Figure S1).

3.3. Estimate of the Viscosity of the Friction Melts

The viscosity η of the friction melt (i.e., suspension = melt + clasts) at $T = 1250$°C for GFB and $T = 1050$°C for GB (see section 3.2) sheared at the steady state at $\sigma_n = 20$ MPa and $V = 3$ m s^{-1} was estimated with the viscosity model of *Costa et al.* [2009]. Melt viscosity was 120 ± 40 Pa s for GFB and 3500 ± 1000 Pa s for GB. Given the measured melt layer of thickness $h \sim 200$ μm for both GB and GFB (Figure 3, thickness of the glass layer at the end of the experiment; see section 4) and the imposed slip rate of 3 m s^{-1}, we estimate the shear stresses as $\tau_{ss} = (\eta\ V/\ h)$. The estimate for τ_{ss_GFB} (1.8 ± 0.6 MPa) is compatible with the steady state shear stress experimental measurements (~1.7 MPa), whereas the estimate for τ_{ss_GB} (33 ± 18 MPa) is not compatible with the experimental measurements (~2.6 MPa) (Figure 2b).

4. Discussion

Mechanical data indicate that the peak friction is independent of the lithology and is compatible with Byerlee's law [*Byerlee*, 1978] (Figure 2a). Conversely, under seismic deformation conditions, an initial fraction of interstitial glass in the rock groundmass strongly influences both the friction decay with slip (GB had a shorter D_w than GFB, Figure 2d) and the steady state friction (GB had higher steady state friction than GFB, Figures 2b and 2c).

4.1. Friction Decay With Slip

Experiments performed on mafic rocks (gabbro and peridotite) under similar conditions ($1 < \sigma_n < 20$ MPa and $1 < V < 6$ m s^{-1}) as ours distinguished two stages of weakening [*Tsutsumi and Shimamoto*, 1997; *Hirose and Shimamoto*, 2005; *Del Gaudio et al.*, 2009; *Niemeijer et al.*, 2011]. First (initial) weakening was associated to flash heating at the asperity contacts, second weakening resulted from bulk melting and lubrication of the slipping zone. Flash heating of the asperities is a local scale process mainly controlled by the contact stress, a material property of the rock-forming minerals [*Rice*, 2006; *Beeler et al.*, 2008]. Therefore, weakening is dependent on the slip rate and independent of the normal stress [*Rice*, 2006; *Goldsby and Tullis*, 2011]. The two weakening stages are separated by a strengthening stage associated with the formation of discontinuous, low-temperature, highly viscous, clast-rich patches of melt [*Hirose and Shimamoto*, 2005]. However, in the previous experiments [e.g., *Niemeijer et al.*, 2011] specimens were pregrinded after their installation in the rotary shear apparatus and the powder produced during pregrinding was only in part removed from the sliding surface before imposing the velocity function. Instead, in the experiments reported here, the strengthening stage was absent. In our experiments, samples were sheared at high speeds without pregrinding: The absence of powder at the initiation of sliding resulted in extreme shear localization. Given the large acceleration and applied normal stress, we surmise that the bulk temperature increase was so abrupt that flash heating and weakening (operating at the asperity scale) was buffered by the formation of viscous melt patches in the slipping zone: This resulted in the absence of two well-defined weakening stages. Consistently, the dependence of the weakening distance with both normal stress and slip rate (i.e., with the power $\sigma_n\ V$ dissipated on the samples, Figure 2d) is suggestive of a bulk (sliding surface) rather than of a local (asperity scale) thermally

activated mechanism. Theoretical models predict a critical distance D_w at which the "bulk" surface melting temperature is reached [*Nielsen et al*., 2008, equation (23)]:

$$D_w = \frac{8\kappa}{V}\frac{\left(\rho(L + c_p(T_m - T_i)\right)^2}{\left(\tau_p\right)^2}. \quad (1)$$

where κ, ρ, c_p, and L are thermal diffusivity, rock density, specific heat capacity, and latent heat, respectively; T_i and T_m are the initial and melting temperature of the rock, respectively. T_m is estimated around 1250°C for GFB. Instead, in the case of the GB sample, the initial fraction of interstitial glass, given its amorphous state, results in thermal softening of the sliding surfaces at lower temperatures than those needed to melt the crystalline rock: GB switches from the solid to the liquid state (glass transition temperature T_g) without the exchange of latent heat of melting ($L = 0\,\mathrm{J\,kg^{-1}}$ in equation 1). T_g depends on the chemical composition of the melt and the water content: T_g ~500°C for a phonolytic glass containing between 0.6 and 3 wt % (if GB water is only contained in the interstitial glass fraction) volatiles [*Giordano et al*., 2005]. Replacing T_m with T_g in equation 1 results in a D_w about 3 times smaller for GB than for GFB, which corresponds to our experimental results (Figure 2d).

4.2. Steady State Friction

Brown and Fialko [2012] and *Nielsen et al*. [2008, 2010] showed the steady state friction in the presence of frictional melt are compatible with the shear of a viscous thin melt layer (melt strength) whose viscosity, thickness, and slip velocity are dynamically determined.

The τ_{ss} estimates based on melt viscosity calculations are consistent with the experimental measurements for GFB but not for GB (section 3.3). The discrepancy can be explained by the following:

1. Overestimation of the effective viscosity. The viscosity of the melt at the steady state depends mainly on chemical composition, clast fraction, temperature distribution within the slip zone [*Lavallée et al*., 2012; *Costa et al*., 2009], and vesicle fraction. In the 30 to 60% interval of clast fraction in volume, the strength of clast-bearing melt evolves from that of a liquid with solid inclusions, to that of a solid with liquid inclusions [*Costa*, 2005; *Costa et al*., 2009; *Mader et al*., 2013] inducing an increase in viscosity of several orders of magnitude. Accordingly, the effective viscosity should be at least 10 times higher in GB frictional melt than in GFB melt, given the difference in clast volume fraction (~50 ± 4% versus ~25 ± 4%, respectively). However, the *Costa et al*. [2009] viscosity model neglects the non-Newtonian rheology of a clast-laden suspension at high strain rates [*Del Gaudio et al*., 2013] and the effect of the vesicles. Vesicles reduce the viscosity of a clast-rich melt by obstructing clast-clast interaction [*Llewellin et al*., 2002]. Therefore, in our experiments, the viscosity may be substantially lower than predicted by the model of *Costa et al*. [2009].
2. Uncertainty on the thickness of the melt layer. Melt strength (or resulting friction) is proportional to the effective viscosity (point a) and inversely proportional to the thickness of the sheared melt layer. Layer thickness results from the melt production versus melt extrusion rate [*Nielsen et al*., 2008]. But the thickness (~ 200 μm) was measured at the end of the experiment when the cooling melt was still under load and partially extruded: It was not possible to measure the melt thickness in situ during the experiment.

Summarizing, the overestimation of the effective viscosity by the *Costa et al*. [2009] model (previous point a) and the uncertainty on the thickness of the effective sheared layer during the experiment (point b) explains why the steady state shear stress values obtained for GBs are only 40 to 50% higher than those obtained for GFBs, as opposed to the factor of 10 predicted by the value of the effective viscosity alone. We also note that the normal stress and slip rate dependences of both rocks are similar for the steady state shear stress (Figure 2b). These nonlinear dependences are typical of melt lubrication [*Persson*, 2000] and predicted by the theoretical model proposed by *Nielsen et al*. [2008], where $\tau_{ss} = C\,\sigma_n^{0.25}$ (C is a factor including the velocity dependence, melt viscosity, and sample size).

4.3. Geophysical Implications

The above observations (sections 4.1 and 4.2) imply that nucleation and propagation of a rupture in basaltic rocks is facilitated by the presence of interstitial glass. In a simple slip-weakening friction model, the fracture energy G is given by [*Andrews*, 1976]

$$G = \frac{1}{2}\left(\tau_p - \tau_{ss}\right) D_w \quad (2)$$

In our experiments we measured extremely low steady state values of shear stress $\tau_{ss\_GB} \approx 2$ MPa and $\tau_{ss\_GFB} \approx 1$ MPa under normal stresses up to 40 MPa. However, the peak shear stress remained high in both GB and GFB, obeying

Byerlee's law with a friction coefficient of ~0.6 (Figure 2a). This implies an almost total strength drop so that the contribution of τ_{ss} to G is negligible. As a consequence the threefold increase in weakening distance ($D_{w\_GB} \approx 1/3\ D_{w\_GFB}$) reflects on an equivalent increase of fracture energy in the absence of glass. Furthermore, the critical length L_c for spontaneous rupture propagation is [*Scholz*, 2002, p. 187]

$$L_c = \frac{C\,M\,\left(\tau_p - \tau_{ss}\right)\,D_w}{\left(\tau_0 - \tau_{ss}\right)^{22}} \tag{3}$$

where C is a dimensionless factor (depending on fault geometry and Poisson ratio), M is the shear stiffness, and τ_0 the preshear stress acting on the fracture (D_w here is the weakening distance defined by [*Ida*, 1972]). Since τ_{ss_GB} and τ_{ss_GFB} are both negligible, equation 3 implies that L_c is 3 times smaller in GB than in GFB under identical conditions of initial stress (provided that the product $M\ C$ remains unchanged). Along the same lines, for a given nucleation length L_c dynamic rupture will initiate under an initial stress τ_0 about $\sqrt{3}$ times smaller in GB than in GFB, ceteris paribus. Under similar conditions, earthquake rupture will be facilitated by the presence of interstitial glass in basaltic rock.

5. Conclusions

The steady state shear stress value measured in the GB is relatively higher than the value measured in GFB (equivalent friction coefficients of ~ 0.21 in GB as opposed to ~ 0.15 in GFB). The difference in steady state stress may be related to the large crystal fraction present in GB frictional melt. However, the residual steady state stress is in all cases extremely small and would not significantly affect the stress drop under dynamic slip. On the other hand, an abrupt and large decrease in friction at the initiation of slip is observed for the GB samples, implying that glass-bearing rocks have a very short weakening distance and reduced fracture energy. The extremely unstable frictional behavior of GB may be related to the thermal softening occurring at the glass transition temperature (T_g ~ 500°C), which is lower than the bulk melting temperature (T_m ~ 1250°C) of the GFB. Due to the fracture energy decrease, the presence of an initial fraction of interstitial glass will facilitate rupture initiation and propagation in earthquakes.

Acknowledgments

This work was funded by the European Research Council Starting Grant project 205175 USEMS. We thank Domenico Mannetta, Leonardo Tauro, and Elena Masiero for thin-section preparation and Piergiorgio Scarlato for laboratory support. B.G. and P.A. thank the Laboratoire Géosciences Montpellier and INSU (program ALEAS 2013) for their financial support. We are grateful to Jean-Marie Dautria for providing basalt samples. We thank Chris Marone and one anonymous reviewer for their thoughtful comments.

The Editor thanks Chris Marone and an anonymous reviewer for their assistance in evaluating this paper.

References

Andrews, D. J. (1976), Rupture velocity of plane strain shear cracks, *J. Geophys. Res.*, *81*(32), 5679–5687, doi:10.1029/JB081i032p05679.

Beeler, N. M., T. E. Tullis, and D. L. Goldsby (2008), Constitutive relationships and physical basis of fault strength due to flash heating, *J. Geophys. Res.*, *113*, B01401, doi:10.1029/2007JB004988.

Brown, K. M., and Y. Fialko (2012), "Melt welt" mechanism of extreme weakening of gabbro at seismic slip rates, *Nature*, *488*, 638–41.

Byerlee, J. (1978), Friction of rocks, *Pure Appl. Geophys.*, *116*, 615–626.

Costa, A. (2005), Viscosity of high crystal content melts: Dependence on solid fraction, *Geophys. Res. Lett.*, *32*, L22308, doi:10.1029/2005GL024303.

Costa, A., L. Caricchi, and N. A. Bagdassarov (2009), Model for the rheology of particle bearing suspensions and partially molten rocks, *Geochem. Geophys. Geosyst.*, *10*, Q03010, doi:10.1029/2008GC002138.

Del Gaudio, P., G. Di Toro, R. Han, T. Hirose, S. Nielsen, T. Shimamoto, and A. Cavallo (2009), Frictional melting of peridotite and seismic slip, *J. Geophys. Res.*, *114*, B06306, doi:10.1029/2008JB005990.

Del Gaudio, P., G. Ventura, and J. Taddeucci (2013), The effect of particle size on the rheology of liquid-solid mixtures with application to lava flows: Results from analogue experiments, *Geochem. Geophys. Geosyst.*, *14*, 2661–2669, doi:10.1002/ggge.20172.

Di Toro, G., T. Hirose, S. Nielsen, and T. Shimamoto (2006), Relating high-velocity rock-friction experiments to coseismic slip, in *Earthquakes: Radiated Energy and the Physics of Faulting*, *Geophys. Monogr. Ser.*, vol. 170, edited by R. Abercrombie et al., pp. 121–134, AGU, Washington, D. C.

Di Toro, G., et al. (2010), From field geology to earthquake simulation: A new state-of-the-art tool to investigate rock friction during the seismic cycle (SHIVA), *Rend. Fis. Acc. Lincei*, *21*, 95–114.

Di Toro, G., R. Han, T. Hirose, N. De Paola, S. Nielsen, K. Mizoguchi, F. Ferri, M. Cocco, and T. Shimamoto (2011), Fault lubrication during earthquakes, *Nature*, *471*(7339), 494–498.

Giordano, D., A. R. L. Nichols, and D. B. Dingwell (2005), Glass transition temperatures of natural hydrous melts: A relationship with shear viscosity and implications for the welding process, *J. Volcanol. Geotherm. Res.*, *142*, 105–118.

Giordano, D., J. K. Russell, and D. B. Dingwell (2008), Viscosity of magmatic liquids: A model, *Earth Planet. Sci. Lett.*, *271*, 123–134.

Goldsby, D. L., and T. E. Tullis (2011), Flash heating leads to low frictional strength of crustal rocks at earthquake slip rates, *Science*, *334*, 216–218.

Han, R., T. Hirose, and T. Shimamoto (2010), Strong velocity weakening and powder lubrication of simulated carbonate faults at seismic slip rate, *J. Geophys. Res.*, *115*, B03412, doi:10.1029/2008JB006136.

Hirose, T., and T. Shimamoto (2005), Growth of molten zone as a mechanism of slip weakening of simulated faults in gabbro during frictional melting, *J. Geophys. Res.*, *110*, B05202, doi:10.1029/2004JB003207.

Ida, Y. (1972), Cohesive force across the tip of a longitudinal-shear crack and Griffith specific surface energy, *J. Geophys. Res.*, *77*(20), 3796–3800.

Lavallée, Y., T. M. Mitchell, M. J. Heap, T. Hirose, and D. B. Dingwell (2012), Experimental generation of volcanic pseudotachylites: Constraining rheology, *J. Struct. Geol.*, *38*, 222e233.

Llewellin, E. W., H. M. Mader, and S. D. R. Wilson (2002), The constitutive equation and flow dynamics of bubbly magmas, *Geophys. Res. Lett.*, *29*, 2170, doi:10.1029/2002GL015697.

Mader, H. M., E. W. Llewellin, and S. P. Mueller (2013), The rheology of two-phase magmas: A review and analysis, *J. Volcanol. Geotherm. Res.*, *234*, 135–158.

Mizoguchi, K., T. Hirose, T. Shimamoto, and E. Fukuyama (2006), Moisture-related weakening and strengthening of a fault activated at seismic slip rates, *Geophys. Res. Lett.*, *33*, L16319, doi:10.1029/2006GL026980.

Nielsen, S., G. Di Toro, T. Hirose, and T. Shimamoto (2008), Frictional melt and seismic slip, *J. Geophys. Res.*, *113*, B01308, doi:10.1029/2007JB005122.

Nielsen, S., P. Mosca, G. Giberti, G. Di Toro, T. Hirose, and T. Shimamoto (2010), On the transient behaviour of frictional melt during seismic slip, *J. Geophys. Res.*, *115*, B10301, doi:10.1029/2009JB007020.

Nielsen, S., E. Spagnuolo, and M. Violay (2012), The ultimate sample preparation for rotary shear experiments. Rapporti tecnici INGV, (http://istituto.ingv.it/l-ingv/produzione-scientifica/rapporti-tecnici-ingv/numeri-pubblicati-2012).

Niemeijer, A., G. Di Toro, S. Nielsen, and F. Di Felice (2011), Frictional melting of gabbro under extreme experimental conditions of normal stress, acceleration, and sliding velocity, *J. Geophys. Res.*, *116*, B07404, doi:10.1029/2010JB008181.

Persson, B. N. J. (2000), *Sliding Friction*, pp. 515, Springer, Berlin.

Rice, J. R. (2006), Heating and weakening of faults during earthquake slip, *J. Geophys. Res.*, *111*, B05311, doi:10.1029/2005JB004006.

Scholz, C. H. (2002), *The Mechanics of Earthquakes and Faulting*, 2nd ed., Cambridge Univ. Press, Cambridge.

Shimamoto, T., and A. M. Lin (1994), Is frictional melting equilibrium or nonequilibrium melting?, *Struct. Geol. (J. Tectonic Res. Group Jpn.)*, *39*, 79–84.

Tsutsumi, A., and K. Mizoguchi (2007), Effect of melt squeezing rate on shear stress along a simulated fault in gabbro during frictional melting, *Geophys. Res. Lett.*, *34*, L21306, doi:10.1029/2007GL031565.

Tsutsumi, A., and T. Shimamoto (1997), High-velocity frictional properties of gabbro, *Geophys. Res. Lett.*, *24*(6), 699–702.

Violay, M., B. Gibert, D. Mainprice, B. Evans, P. Azais, and P. A. Pezard (2012), An experimental study of the brittle-ductile transition of basalt at oceanic crust pressure and temperature conditions, *J. Geophys. Res.*, *117*, B03213, doi:10.1029/2011JB008884.